J. Braz. Chem. Soc., Vol. 22, No. 9, 1709-1717, 2011.
Printed in Brazil - ©2011 Sociedade Brasileira de Química
0103 - 5053 $6.00+0.00

Article

Ethanol Electrooxidation using $Ti/(RuO_2)_{(x)}$ $Pt_{(1-x)}$ Electrodes Prepared by the Polymeric Precursor Method

R. G. Freitas,[a] L. F. Q. P. Marchesi,[a] M. R. Forim,[a] L. O. S. Bulhões,[a,b] E. C. Pereira,[a] M. C. Santos[c] and R. T. S. Oliveira*[,d]

[a]*Departamento de Química, Universidade Federal de São Carlos, CP 676, 13565-905 São Carlos-SP, Brazil*

[b]*CENIP, Centro Universitário Central Paulista, Rua Miguel Petroni, 5111, 13563-470 São Carlos-SP, Brazil*

[c]*LEMN, Centro de Ciências Naturais e Humanas, Universidade Federal do ABC, Rua Santa Adélia, 166, Bairro Bangu, 09210-170 Santo André-SP, Brazil*

[d]*Instituto de Ciências Biológicas e Naturais, Universidade Federal do Triângulo Mineiro, Av. Frei Paulino, 30, Bairro Abadia, 38025-180 Uberaba-MG, Brazil*

Este trabalho descreve um estudo detalhado da oxidação eletroquímica de etanol sobre eletrodos de $Ti/(RuO_2)_{(x)}Pt_{(1-x)}$ com várias composições, preparados pelo método de precursores poliméricos. Os resultados obtidos usando voltametria cíclica e cronoamperometria mostraram que a melhor composição dos eletrodos de $Ti/(RuO_2)_{(x)}Pt_{(1-x)}$ para os processos de oxidação do CO e do etanol é $Ti/(RuO_2)_{(0.5)}Pt_{(0.5)}$. Nessa composição, a oxidação do CO e do etanol ocorreram em 380 mV e 220 mV mais negativos do que em Ti/Pt, respectivamente. Por outro lado, observou-se um aumento de 2.5 vezes na densidade de corrente para a oxidação do etanol sob potencial constante. Análises de HPLC *in situ* mostraram que os eletrodos de $Ti/(RuO_2)_{(0.5)}Pt_{(0.5)}$ produziram baixas quantidades de ácido acético comparadas com aquelas quantidades geradas pelos eletrodos de Ti/Pt ou Pt policristalina. Além disso, um produto que não é comum a partir da oxidação do etanol foi observado em eletrodos com maior teor de RuO_2: o acetato de etila. Finalmente, os dados de impedância mostraram que os eletrodos com a composição $Ti/(RuO_2)_{(0.5)}Pt_{(0.5)}$ apresentaram menores resistências de transferência de carga, entre as composições investigadas.

This work describes a detailed study of the ethanol electrooxidation on $Ti/(RuO_2)_{(x)}Pt_{(1-x)}$ electrodes using several compositions prepared by the polymeric precursor method. The results obtained using cyclic voltammetry and chronoamperometry showed that the best composition of $Ti/(RuO_2)_{(x)}Pt_{(1-x)}$ electrodes for CO and ethanol oxidation processes is $Ti/(RuO_2)_{0.50}Pt_{0.50}$. On this electrode composition the onset of CO and the ethanol oxidation occurred at 380 mV and 220 mV more negative than on Ti/Pt, respectively. Besides, there was an increase of 2.5-fold in the current density for ethanol electrooxidation under constant potential polarization. The $Ti/(RuO_2)_{0.50}Pt_{0.50}$ electrodes produced lower amount of acetic acid compared to Ti/Pt and polycrystalline Pt electrodes using *in situ* HPLC spectrometric analysis. Also, a non common product from ethanol oxidation could be observed on higher RuO_2 loads: ethyl acetate. Finally, the impedance data showed that $Ti/(RuO_2)_{0.50}Pt_{0.50}$ electrode composition had the smallest charge transfer resistance for ethanol oxidation among those compositions investigated.

Keywords: ethanol electrooxidation, polymeric precursor method, CO electrooxidation, eletrocatalysis, *in situ* HPLC

Introduction

Fuel cells are widely recognized as very attractive devices to obtain directly electric energy from the combustion of a chemical product. In the last decades, much attention has been devoted to the study of the electrooxidation of small organic molecules, due to their possible utilization as fuels in direct organic fuel cell (DOFCs) devices.[1,2] Ethanol has emerged as important choice due to its low toxicity and volatility together with a higher energy density than methanol (8.01 kWh kg^{-1} *versus* 6.09 kWh kg^{-1}).[3] Other important considerations for choosing ethanol are its low

*e-mail: robson@icbn.uftm.edu.br

price and transportability. Among the published reports on proton exchange membrane fuel cells (PEMFC) with alcohol as fuel, the direct ethanol fuel cell (DEFC) is promising especially for the application in devices such as electric vehicles, mobile telephone and laptops.[4] For maximum energy recovery from ethanol, 12 electrons *per* molecule, it is necessary to achieve its complete oxidation to CO_2 which requires the C–C bond cleavage and oxidation of intermediate species that strongly adsorb on Pt electrodes.[5,6] The increase of the electroactivity for ethanol oxidation reaction and its complete oxidation into carbon dioxide, is a hard challenge.[7] Platinum surface is known to be rapidly poisoned by strongly adsorbed species coming from the dissociation of organic molecules. Therefore, this oxidation on Pt is sluggish, especially at low temperatures.[4]

Numerous papers on ethanol electrooxidation have been devoted on the development of appropriated catalysts.[5-14] Binary, ternary alloys and multilayers of noble metals have been applied for ethanol electrooxidation.[6-17] New materials are important in order to decrease the irreversible adsorption of such intermediates during the electrocatalysts of ethanol oxidation. Different electrocatalysts preparation methods have been proposed for the obtainment of electrodes for this task.[18-21] Nanostructured metal oxides containing Pt particles, such as ruthenium oxides, are very attractive as electrocatalysts for electrooxidation of small organic molecules, due to the capability to adsorb OH and decreasing the adsorption of intermediates generated during the reaction.[12-22] Electrochemical impedance spectroscopy (EIS) is a powerful technique to propose models, which describe these reactions.[23-28] The model describes the different contribution of the process occurring during the reaction.[23-27]

Considering the exposed above, the aim of this work is to investigate the electrocatalytical activity of Ti/$(RuO_2)_{(x)}Pt_{(1-x)}$ electrodes prepared by the polymeric precursor method (PPM) toward CO and ethanol electrooxidation using cyclic voltammetry and chronoamperometric experiments. Besides, the characteristics of electrocatalytical activity of the electrodes for ethanol electrooxidation reaction at different potentials using impedance spectroscopy were determined. The intermediates products were elucidated using high performance liquid chromatography (HPLC) in terms of reaction product distribution depending on the anode catalyst.

Experimental

Electrodes preparation

The electrodes were prepared using a 10 × 5.0 × 0.5 mm titanium plate as substrate (TiBrasil 99.7%). The substrates were treated by sandblasting followed by a chemical treatment in hot aqueous oxalic acid 10% (m/m) for 30 min. After the chemical treatment, the substrates were washed with Millie-Q water and dried at 130 °C.

The precursor solution was prepared dissolving citric acid (Synth) in ethylene glycol (Merck) at 60 °C. In this solution, $H_2PtCl_6 \cdot 7H_2O$ (Aldrich) and $RuCl_3 \cdot 3H_2O$ (Aldrich) was added maintaining the total metal amount constant in the following ratio: 1:62.5:290. Different Pt content were used to prepare the Ti/$(RuO_2)_{(x)}$ $Pt_{(1-x)}$ electrodes *i.e.*, x = 1.0, 0.875, 0.75, 0.50 and 0.

The precursor solution was painted with a brush onto the support (Ti) and the material was initially treated at 130 °C for 10 min to eliminate water, 250 °C for 20 min and 400 °C for 30 min to eliminate the organic materials producing the composite films. This procedure was repeated ten times and, at the end, the total electrode mass was close to 0.1 mg cm^{-2}. After the last thermal treatment, the electrode was cooled using 5 °C min^{-1} until room temperature. All electrodes were both fabricated in static air atmosphere. The microstructure of the electrodes was characterized by X-ray diffraction elsewhere.[20]

Electrodes characterization

The electrochemical characterization was accomplished using a potentiostat/galvanostat EG&G PARC model 263A. All the electrochemical experiments were carried out at 25 °C. The voltammetric curves were measured in 0.1 mol L^{-1} $HClO_4$ solution in the potential range between 0.05 and 1.4 V (*vs.* a reversible hydrogen electrode, RHE). A Pt plate was used as auxiliary electrode. The ethanol electrooxidation was investigated in a 0.1 mol L^{-1} $HClO_4$ solution containing 0.5 mol L^{-1} ethanol by means of cyclic voltammetry (CV) and chronoamperometry (CA). Prior to the experiments, the solutions were deaerated with N_2 for 30 min. EIS data were measured using an Autolab/PGSTAT 302N potentiostat at frequencies between 10 kHz to 0.01 Hz with 12 points *per* decade. The amplitude of the sinusoidal potential signal was 5 mV. Initially, the electrodes were polarized during 5 min prior the measurement to reach the steady state condition and then, the EIS experiment was started. The fitting data were done with software Zview 2.6.[29]

HPLC analysis

Electrolysis was performed in a solution of 0.5 mol L^{-1} ethanol in 0.1 mol L^{-1} $HClO_4$ at room temperature in a two-compartment glass cell separated by a fritted glass tube on Ti/$(RuO_2)_{(x)}$ $Pt_{(1-x)}$ as working electrodes. Reference and counter electrodes were described previously. Electrolysis

samples were analyzed by extracting 500 μL from the electrochemical cell. An Agilent-1200 Series automated high perform liquid chromatograph compromising a UV detector at 202 nm wavelengths was used. The column used was a C18 (10 cm × 4.6 mm × 3 μm, 100 A) serial number 100040 from Regis Rexchrom. The mobile phase (0-50% linear gradient of acetonitrile in 0.1% H_3PO_4) was applied during 8 min along thermal gradient until 35 °C. Flow rate was 0.5 mL min^{-1} and the injection volume was 20 μL. The relative concentration of the products acetic acid and acetaldehyde was calculated by considering the peak area. In all experiments 0.1 mol L^{-1} $HClO_4$ was prepared from suprapure chemical (Merk) and millipore water. Ethanol was of spectroscopic grade (Aldrich), acetaldehyde A.C.S. and reagent and acetic acid (Aldrich) were used as standards for HPLC.

Results and Discussion

Characterization of the Ti/$(RuO_2)_{(x)}Pt_{(1-x)}$ electrodes

Electrochemical characterization

The voltammetric profiles of Ti/$(RuO_2)_{(x)}Pt_{(1-x)}$ prepared by PPM with different compositions are presented in Figure 1.

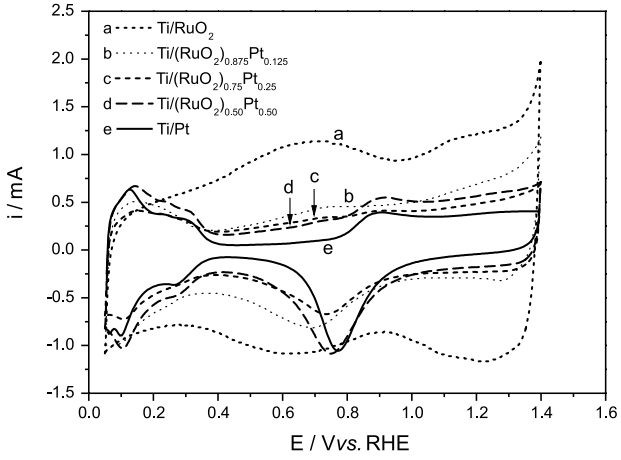

Figure 1. Cyclic voltammograms of Ti/$RuO_{2(x)}Pt_{(1-x)}$ electrodes in 0.1 mol L^{-1} $HClO_4$. ν = 50 mV s^{-1}, T = 25 °C.

The feature of these voltammetric profiles are similar to those related in the literature, where the authors worked with binary composition of Pt and RuO_2 electrodes prepared by alkoxide route[18] and Pt by PPM.[19-21] Dobholfer *et al.*[30] proposed that RuO_2 electrodes present redox transitions between Ru^{2+} to Ru^{6+} in the potential range between 0.4 and 1.4 V (*vs.* RHE) in acidic medium,[30] which was confirmed using EQCN method.[31,32] The peak at 0.75 V could be associated with the redox transition of Ru^{3+} to Ru^{4+}, and the peak at 1.1 V to Ru^{4+} to Ru^{6+}, but this last one, is a sum of this redox process of RuO_2 and a peak that appears in the voltammetric profile of Ti/Pt. In these voltammetric profiles showed in Figure 1, we could not observe the transition of Ru^{2+} to Ru^{3+}, once this process occurs in the hydrogen adsorption region.[33] The current response in the hydrogen region shows a clear relation with the Pt content, the peaks for H adsorption being better defined as the RuO_2 content decreases. The form of this voltammograms is, in principle, in agreement with the relative Pt:Ru molar ratio. It is also observed in Figure 1 that increasing the Pt load in the electrode, there is a decrease in the capacitive currents between 0.4 and 1.4 V. In order to compare the electrocatalytical properties for bimetallic materials, a Ti/Pt electrode was prepared. The characteristic redox process for Ti/Pt electrode can be viewed in Figure 1 for that sample: (*i*) adsorption and desorption of hydrogen UPD on Pt (0.05 to 0.4 V); (*ii*) anions adsorption in the double layer region (0.4 to 0.9 V), and formation and reduction of the superficial PtO and PtO_2, between (0.9 to 1.4 V) and (1.4 to 0.5 V).

Electrocatalytical activity

The reaction of CO as probe molecule on electrocatalytic materials, has essentially been focused on elucidating the role of an adsorbed poison for the electrooxidation of small organic molecules on transition metals and alloys and therefore, identifying the best CO-tolerant catalysts.[34-39] Hence this reaction can be used to deep understanding the ethanol oxidation processes on Ti/$(RuO_2)_{(x)}Pt_{(1-x)}$ electrocatalyst, the voltammetric profiles of CO electrooxidation onto Ti/$(RuO_2)_{(x)}Pt_{(1-x)}$ with different Pt load are presented in Figure 2 and compared to Ti/Pt electrode.

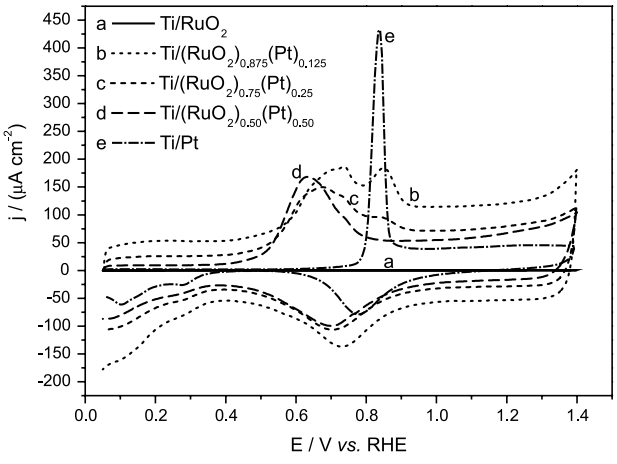

Figure 2. Cyclic voltammograms obtained for the oxidative stripping of a CO monolayer on Ti/$RuO_{2(x)}Pt_{(1-x)}$ electrodes in 0.1 mol L^{-1} $HClO_4$. ν = 50 mV s^{-1}, T = 25 °C.

It can be seen that CO molecules are not adsorbed on Ti/RuO_2 electrodes and consequently there are no anodic currents related to this reaction. Among the electrodes that have Pt in its composition, the smallest CO oxidation charge was observed for Ti/$(RuO_2)_{(x)}Pt_{(1-x)}$ (x = 0.875), which has been the smallest Pt load investigated in this work. This effect can be related to a small OH nucleation rates on Pt and RuO_2 sites distributions. According to MacDougall *et al.*[40] in the case of the CO_{ads} oxidation reaction, the presence of RuO_2 in combination with poorly distributed Pt sites on the catalyst surface was found to result in a significant slower CO_{ads} oxidation reaction. The formation of OH species on Ru sites are needed for the CO_{ads} to CO_2 oxidation reaction according to the bifunctional mechanism.

One important challenge is to prepare electrocatalysts which changes the small organic molecules oxidation potential toward more negative values, compared to Pt_{pc} electrodes. In this sense, the electrocatalytical data presented herein are compared to Ti/Pt electrode. All the electrodes studied changed the CO electrooxidation potential to more negative values on both: the onset of the oxidation process and the peak potential. Besides, differently that was observed for Ti/Pt (one defined and sharp peak for CO oxidation) on Ti/$(RuO_2)_{(x)}Pt_{(1-x)}$ electrodes, at least two anodic peaks current density appear. It must be stress out that, whole current values were normalized by the surface area obtained by CO stripping procedure. This parameter can be calculated using the oxidation charge of one CO_{ads} monolayer.[53] When discussing the reason for the catalytic effect of Ti/$(RuO_2)_{(x)}Pt_{(1-x)}$, the bi-functional mechanism is invoked.[41] Koper *et al.*[42] found that an enhancement in the electrocatalytical effect is possible over a mechanism between CO adsorbed on Pt and OH adsorbed at Ru. Therefore, it can be written as:

$$Pt–CO_{ads} + Ru–OH_{ads} \rightarrow CO_2 + H^+ + e^- \quad (1)$$

For this reason, a better distribution for RuO_2 and Pt sites, increase the electrocatalytical effect and, explain the better activity of Ti/$(RuO_2)_{(x)}Pt_{(1-x)}$ (x = 0.5) compared to Ti/Pt electrode. Another point of view, the content of Ru may change the chemical properties of Pt atoms in the surface. If the effect is that CO is bound more weakly, the CO coverage should be smaller and hence the CO poisoning effect became weaker.[43] So, the change of potential towards more negative values could be associated to both electronic and bifunctional effects, where the alloying metal may be better than Ti/Pt electrodes at dissociating water and providing OH groups to react with the CO at Pt sites, thus decreasing the CO coverage. The possible explanation it is a better dispersion of Pt on RuO_2 matrix oxide and it is related to electronic effect and bifunctional mechanism as described above.[44,45] The CO electrooxidation peak potential displacement were 115, 160 and 230 mV toward more negative potentials to Ti/$(RuO_2)_{(x)}Pt_{(1-x)}$ (for x = 0.875, 0.75 and 0.50) electrodes, respectively, compared with Ti/Pt electrode. Furthermore, the onset of CO electrooxidation process is 380 mV more negative for Ti/$(RuO_2)_{0.50}Pt_{0.50}$ electrodes than on Ti/Pt electrodes. Still analyzing the Figure 2, it can be observed two peaks in the CO electrooxidation. Maillard *et al.*[46] attributed these peaks to Pt nanoparticles of different sizes and discussed CO stripping shape as a function of the particle size distribution.

In Figure 3a, the voltammetric profiles for ethanol electrooxidation on Ti/$(RuO_2)_{(x)}Pt_{(1-x)}$ and Ti/Pt electrodes are compared. Ethanol oxidation on polycrystalline Pt is characterized by the presence of two current density peaks at 0.9 and 1.23 V.[47] However, the peaks potential on Figure 3 are displaced and it is possible related to some differences on the mechanism.

The anodic shoulder related to some parallel electrochemical process observed in the cyclic voltammogram

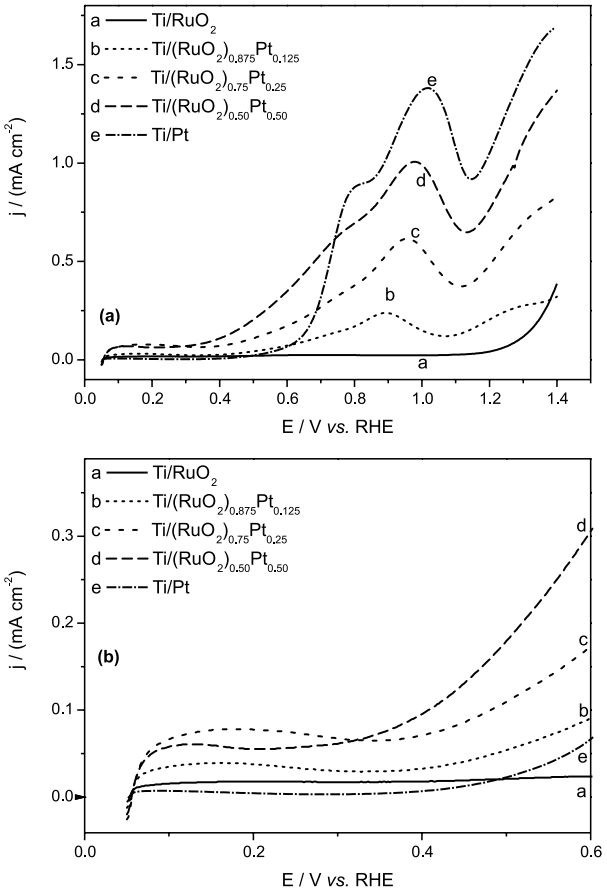

Figure 3. Cyclic voltammograms obtained for (a) electrooxidation of 0.5 mol L^{-1} ethanol in 0.1 mol L^{-1} $HClO_4$ and (b) presenting the shifting of the onset potential during ethanol electrooxidation on Ti/$(RuO_2)_{(x)}$ $Pt_{(1-x)}$ electrodes. ν = 50 mV s^{-1}, T = 25 °C.

(region between 0.7 and 0.9 V), which is well defined on Ti/Pt (0.8 V) can be attributed to dehydrogenation of ethanol, which is a slow process on the surface of catalysts at lower potentials.[48] Behm *et al.*[49] had observed the same process studying the ethylene glycol electrooxidation over Pt nanoparticles by DEMS. According to the authors, the process observed in the positive-going scan corresponds to the oxidation of CO_{ads} to CO_2, and a similar shoulder was also observed to glycol aldehyde. The reason for this behaviour is not clear yet and, new spectroscopic experiments will be done in a further work.

The ethanol electrooxidation main peak appears at a potential range where the surface-bonded OH is formed on Ti/Pt electrodes, which is characterized by a steep rise in the current density just after the hydrogen current density peaks during the positive sweep. The formation of OH species has an important role in ethanol oxidation. A two-path mechanism can occur, with formation of strongly CO_{ads} bonded to the Pt substrate and also bulk oxidation.[47] The peaks in the oxide region of Pt in acid solution are caused by production of CO_2 and carboxylic acid. The main products of ethanol oxidation are adsorbed CO, adsorbed CH_3CO, CH_3CHO, CH_3COOH and CO_2, which were detected by *in situ* reflectance spectroscopy and chromatography techniques.[50-52]

Analyzing the ethanol electrooxidation process (Figure 3a), it can be observed that peak potential is displaced 150 mV toward more negative values for Ti/Pt compared to $Ti/(RuO_2)_{0.875}Pt_{0.125}$. Still analyzing the ethanol electrooxidation, we observe that ethanol is not adsorbed on Ti/RuO_2 and therefore there are no currents related to this reaction, as already described for methanol oxidation reaction.[20,32]

Although Ti/Pt electrodes exhibit higher peak current density related to ethanol electrooxidation compared to bimetallic electrodes, in Figure 3b, it is possible to observe that $Ti/(RuO_2)_{0.50}Pt_{0.50}$ electrode presents the beginning of the onset potential for ethanol oxidation displaced in 220 mV towards negative potentials compared to Ti/Pt electrode. It is important to point out that the observed electrocatalytical properties are not an area effect, once all the presented results were normalized by the electroactive surface area related to each electrode.

The comparison of the Ti/Pt and $Ti/(RuO_2)_{(x)}Pt_{(1-x)}$ electrodes under constant-potential polarization of 0.5 V for 15 min in an acid solution containing ethanol are presented in Figure 4.

It is observed that the current density for Ti/RuO_2 and $Ti/(RuO_2)_{0.875}Pt_{0.125}$ falls to negligible values after 2 min of polarization. As expected, the $Ti/(RuO_2)_{0.50}Pt_{0.50}$ electrode exhibited the best results and an increase in current density

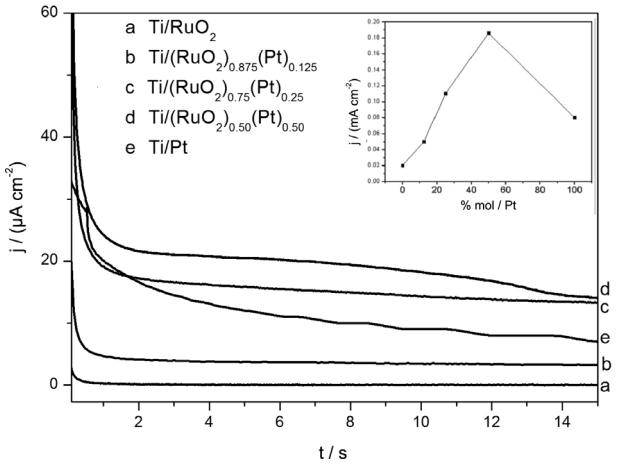

Figure 4. Chronoamperometric measurements for 0.5 mol L^{-1} ethanol in 0.1 mol L^{-1} $HClO_4$ on $Ti/(RuO_2)_{(x)}$ $Pt_{(1-x)}$ electrodes. E_{ox} = 0.5V. T = 25 °C. Inset: optimal ratio of Pt load.

after 15 min toward ethanol oxidation near to 2.5-fold higher than on Ti/Pt electrodes. The $Ti/(RuO_2)_{0.50}Pt_{0.50}$ electrode seems to present a site distribution close to the optimum for ethanol oxidation. RuO_2 concentrations higher than *ca.* 50% cause the decreasing in the current values, this effect can be rationalized in terms of an inhibition of ethanol adsorption, which is probably due to the diminution of Pt sites. In the range of x = 0 and 0.5 (not studied here), Camara *et al.*[53] has founded that for low Ru load, there is no enough Ru sites to OH adsorbed and the catalysis mechanism operate as bifunctional. In that case, a Pt:Ru ratio of 60:40 seems to present a site distribution close to the optimum for ethanol electrooxidation. In this paper, we found a better RuO_2:Pt ratio of 50:50, as can be seem on the inset of Figure 4. This high value is related with morphological and structured factors. It is well known that the addition of foreign metal to Pt catalyst, significantly lowers the overpotential for ethanol electrooxidation reaction through a so-called bifunctional mechanismAn attempt to explain the difference in the behavior of $Ti/(RuO_2)_{(x)}Pt_{(1-x)}$ set of electrodes has been made to determining the reaction product using long-term electrolysis and *in situ* HPLC spectrometric analysis. In order to compare the lowest electrocatalytical activity related to polycrystalline Pt (Pt_{pc}) with the set of binary electrodes, its chromatograms is also exhibit for ethanol oxidation. In Figure 5 it is possible to observe the presence of ethanol, acetic acid, acetaldehyde and some species present in $HClO_4$ acidic medium. The lowest acetic acid retention time compared to acetaldehyde is related to its lower dipole moment 1.74D and 2.7D for acetaldehyde. Also, must be considered the interaction of these species with mobile phase.

Iwasita *et al.*[54] studied the ethanol electrooxidation mechanism using *in situ* FTIR electrochemical spectroscopy. The authors observed that the acetaldehyde formation

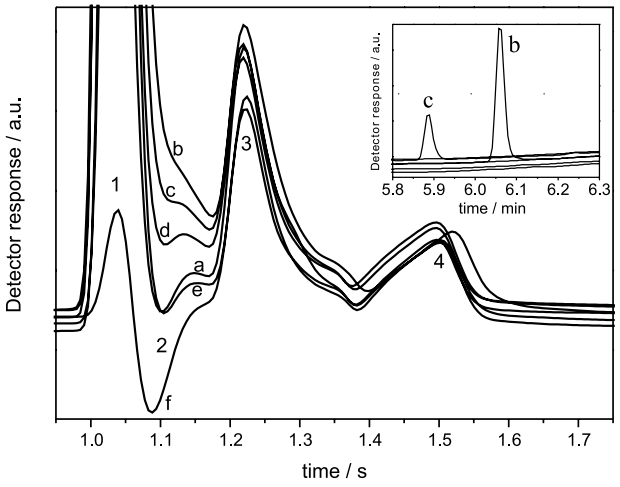

Figure 5. Chromatograms of the 0.5 mol L^{-1} ethanol in 0.1 mol L^{-1} after 30 min electrolysis (E = 0.5V) on a) Ti/RuO_2, b) $Ti/(RuO_2)_{0.875}$ $Pt_{0.125}$, c) $Ti/(RuO_2)_{0.75}$ $Pt_{0.25}$, d) $Ti/(RuO_2)_{0.50}$ $Pt_{0.50}$ e) Ti/Pt and f) polycrystalline Pt electrodes. Ethanol (1), acetic acid (2), acetaldehyde (3), perchloride specie (4). Inset: ethyl acetate.

precedes the acetic acid production. As can be observed on Figure 5, acetaldehyde band (3) is observed for all electrodes almost in the same amount. However, the acetic acid band (2) is observed mainly for non-binary electrodes, such as Pt_{pc} (f), Ti/Pt (e) and Ti/RuO_2 (a). As soon as $Pt:RuO_2$ materials in different amounts is obtained, the selectivity of the ethanol electrooxidation mechanism is changed and acetic acid band is decreased. Finally, on the inset of Figure 5 it is possible to observe on the chromatograms the presence of bands related to ethyl acetate for $Ti/(RuO_2)_{0.875}Pt_{0.125}$ (b) and $Ti/(RuO_2)_{0.75}Pt_{0.25}$ (c). Ethyl acetate production has been observed for ethanol oxidation on Ni, Cu and Ru over polyvinyl chloride,[55] Pt/SiO_2[56] and $PdO/Ce_{0.75}Zr_{0.25}O_2$[57] catalyst and it is a remarkable evidence of changes on the ethanol electrooxidation mechanism for $Ti/(RuO_2)_{(x)}Pt_{(1-x)}$ bimetallic electrodes. The enhancement for ethanol electrooxidation observed previously for $Ti/(RuO_2)_{0.50}Pt_{0.50}$ electrodes, can be a consequence of non ethyl acetate production (observed for RuO_2:Pt 87.5:12.5 and 75:25 molar ration) and lower acetic acid production, maximizing the acetaldehyde production, which is easiest to obtain through the ethanol electrooxidation.

Electrochemical impedance spectroscopy

We investigate two different potentials, 0.5 and 0.9 V, once in these potential values, surface-bonded Pt-OH and PtO are formed on Pt surface, respectively. The study was carried out in two different solutions: the blank solution, in 0.1 mol L^{-1} $HClO_4$, and 0.5 mol L^{-1} ethanol in 0.1 mol L^{-1} $HClO_4$, in order to compare the effect of presence and absence of organic molecules adsorbing onto $Ti/(RuO_2)_{(x)}Pt_{(1-x)}$.

It can be observed the same profile for different $Ti/(RuO_2)_{(x)}Pt_{(1-x)}$ compositions in the presence of ethanol (solution of 0.5 mol L^{-1} ethanol in 0.1 mol L^{-1} $HClO_4$) at 0.9 V, as can be seem in Figure 6. In general, it is observed an equal behavior in the Nyquist plot.

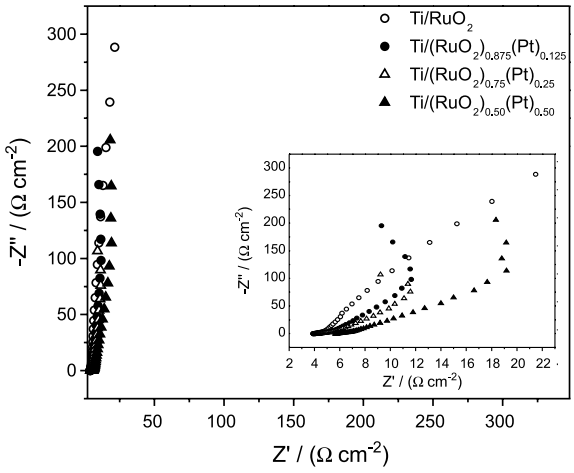

Figure 6. Nyquist plots of EIS for 0.5 mol L^{-1} ethanol in 0.1 mol L^{-1} $HClO_4$ reaction on $Ti/(RuO_2)_{(x)}$ $Pt_{(1-x)}$ electrodes electrochemically polarized at 0.9 V. T = 25 °C.

In a general analysis, at low frequencies, complex plane plot for $Ti/(RuO_2)_{(x)}Pt_{(1-x)}$ at 0.9 V is similar for all the compositions investigated. Nevertheless, analyzing the inset in Figure 6, at high frequencies, an important change in the impedance plots occurs, with reversing loops to the 2nd quadrant, *i.e.*, with the real component of the impedance becoming negative. Complex plane plot like this for methanol electrooxidation were observed for PtRu (1:1 atom ratio) catalyst prepared dispersing it on carbon and supporting onto glassy carbon.[61] This reversed loop to the 2nd quadrant could be related with the passivation of electrode surface,[58] and then, to the PtO formation in this potential.[59] Melnick *et al.*[60] indicated that the passivation of the Pt electrode during methanol electrooxidation is probably due to reversible formation oxide species. Moreover, the electrooxidation of CO_{ads} with OH is very slow, then the passivation at higher potentials can be explained by the formation of a large amount of CO_{ads} and OH on surface of $Ti/(RuO_2)_{(x)}Pt_{(1-x)}$ electrodes. Therefore, the adsorption of ethanol on Pt sites is inhibited due to an increase of coverage of CO_{ads} and OH on Pt sites, leading to the electrooxidation rate is almost no obvious increased. As can be observed in Figure 6, Ti/RuO_2 electrodes does not exhibit loops reversing to the 2nd quadrants, because as explained above, RuO_2 sites neither adsorb organic molecules nor form passivation films onto surface like PtO onto Pt electrodes.[61]

The complex plane plot at 0.5 V in the blank solution is presented in Figure 7a (inset) for different binary

$Ti/(RuO_2)_{(x)}Pt_{(1-x)}$ electrodes, where, as can be seem, there is only a capacitive feature in this case. This behavior is associated to absence of faradaic reactions in this potential, because there is no organic molecules adsorption or other faradaic reaction. The equivalent circuit suitable to fit the experimental data is shown in Figure 7b. This equivalent circuit represents the impedance data for pseudocapacitive behavior with the resistance Rs in series to a non ideal capacitor, *i.e.*, constant phase element (CPE), where does not exist intermediates species adsorbed on the electrode surface. In this model, Rs is the solution resistance and considering the non-homogeneity of the electrode surface, a constant phase element (CPE) is used to replace capacitive element.[62] Table 1 shows the values for each circuit elements.

Table 1. Values obtained to R_s, CPE_T and CPE_P for $Ti/(RuO_2)_{(x)}$ $Pt_{(1-x)}$ electrodes in 0.1 mol L^{-1} $HClO_4$

Element Circuit	Rs / (Ω cm^2)	CPE_T / (F cm^{-2})	CPE_P
	6.195	3.742E-3	0.925

A different behavior can be observed for $Ti/(RuO_2)_{(x)}Pt_{(1-x)}$ electrodes at 0.5 V in ethanol 0.5 mol L^{-1} in $HClO_4$ 0.1 mol L^{-1}. Figures 7a and 7c present the complex plane plot for $Ti/(RuO_2)_{(x)}Pt_{(1-x)}$ electrodes at 0.5 V and the equivalent circuit proposed.

As can be seen in Figure 7a, a large capacitive arc for Ti/RuO_2 reveals a non reaction rate of ethanol dehydrogenation oxidation onto RuO_2 sites, and one can correlate this fact with the large value for the R_{ct} in Table 2 among those electrode compositions investigated: 8.46×10^{11} Ω cm^2. The equivalent circuit that best fit these data was presented in Figure 7c. It is based in R_s in series with the CPE and charge transfer resistance in parallel. It is possible to observe that the arc decrease with the increase of Pt load until $Ti/(RuO_2)_{0.50}Pt_{0.50}$, where is observed a charge transfer resistance of 426.2 Ω cm^2 presented in Table 2. It is proposed in the literature that the slow kinetics is caused by the intermediate CO_{ads} from ethanol dehydrogenation which is strongly adsorbed on Pt sites and block continuous adsorption and dehydrogenation of ethanol molecules. Then the decrease of charge transfer

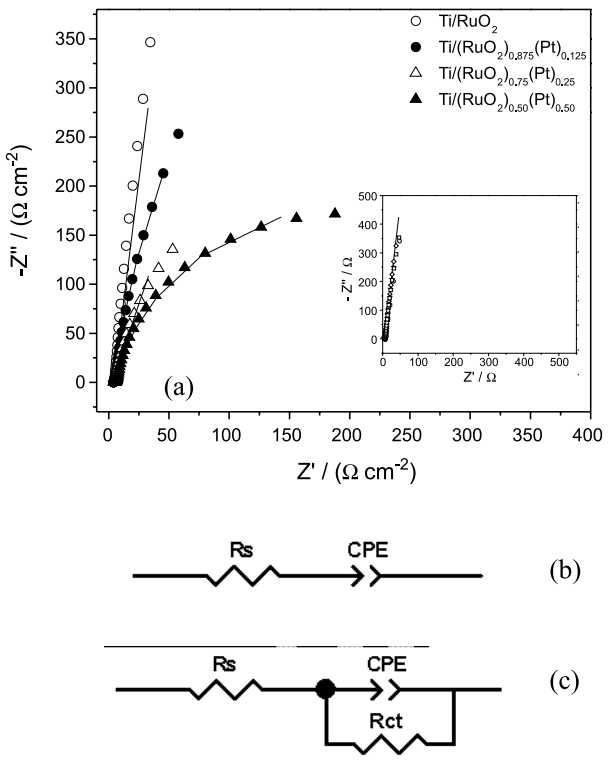

Figure 7. Nyquist plots of EIS for a) 0.5 mol L^{-1} ethanol in 0.1 mol L^{-1} $HClO_4$ and inset: 0.1 mol L^{-1} $HClO_4$ reaction on $Ti/(RuO_2)_{(x)}$ $Pt_{(1-x)}$ electrodes electrochemically polarized at 0.5 V. T = 25 °C. b) Electric circuit analog for the interfacial phenomena proposed and fitted to impedance data in 0.1 mol L^{-1} $HClO_4$ and c) 0.5 mol L^{-1} ethanol in 0.1 mol L^{-1} $HClO_4$.

resistance as Pt content is increased from Ti/RuO_2 to $Ti/(RuO_2)_{0.50}Pt_{0.50}$ can be related to increase in the number of Pt sites able to adsorb organic molecules and also to the presence of RuO_2 sites which can adsorb OH species. These finds are in agreement with those observed in Figures 2, 3 and 4 where $Ti/(RuO_2)_{0.50}Pt_{0.50}$ shows an enhanced catalytical activity.

Conclusions

In this work, it was found that the best composition of the $Ti/(RuO_2)_{(x)}Pt_{(1-x)}$ electrodes prepared by the polymeric precursor method toward CO and ethanol electrooxidation processes is (x = 0.5). The onset of CO oxidation process occurred 380 mV less positive than on Ti/Pt. Furthermore,

Table 2. Values obtained to R_s, CPE_T, CPE_P and R_{ct} for $Ti/(RuO_2)_{(x)}$ $Pt_{(1-x)}$ electrodes in 0.5 mol L^{-1} ethanol + 0.1mol L^{-1} $HClO_4$

Element Circuit	Rs / (Ω cm^2)	CPE_T / (F cm^{-2})	CPE_P	R_{ct} / (Ω cm^2)
RuO_2	4.053	4.59×10^{-3}	0.9352	8.465×10^{11}
RuO_2:Pt (87.5:12.5)	4.285	6.235×10^{-3}	0.8950	4.370×10^{15}
RuO_2:Pt (75:25)	4.489	4.280×10^{-2}	0.8538	3945
RuO_2:Pt (50:50)	6.036	1.6235×10^{-2}	0.9015	426.2

the onset for ethanol oxidation process is 220 mV less positive than on Ti/Pt electrodes. There was an increase of approximately 2.5-fold in the current density for ethanol electroxidation in the chronoamprometric experiments using the Ti/$(RuO_2)_{0.50}Pt_{0.50}$ electrodes. Using *in situ* HPLC spectrometric analysis, it was possible to observe the acetic acid and acetaldehyde as ethanol electrooxidation products. For higher RuO_2 load on binary electrodes, ethyl acetate could be detected. Ti/$(RuO_2)_{0.50}Pt_{0.50}$ electrode has presented the smallest charge transfer resistance (using electrochemical impedance spectroscopy, EIS) among the Ti/$(RuO_2)_{(x)}Pt_{(1-x)}$ electrodes studied herein. With the results obtained in this paper is possible to affirm that RuO_2Pt binary electrodes can be attractive materials for the development of active catalysts for direct ethanol fuel cells.

Acknowledgments

The authors wish to thank the Brazilian research funding institutions CNPq (473151/2008 1), CAPES and FAPESP (05/59992-6, 2010/05555-2 and 03/09933-8).

References

1. Iwasita, T.; Vielstich, W. In *Advances in Electrochemical Sciences and Engineering*; Gersischer, H.; Tobias, C. W., eds., VCH: Weinheim, 1990, vol.1.
2. Parsons, R.; Vandernoot, T.; *J. Electroanal. Chem.* **1988**, *9*, 257.
3. Xu, C.; Shen, P. K.; *J. Power Sources* **2005**, *142*, 27.
4. Wang, Z.; Yin, G.; Zhang, J.; Sun, Y.; Shi, P.; *J. Power Sources* **2003**, *37*, 160.
5. Chang, S. C.; Leung, L. W. H.; Weaver, M. J.; *J. Phys. Chem.* **1990**, *94*, 6013.
6. Iwasita, T.; *J. Braz. Chem. Soc.* **2002**, *13*, 401.
7. Pacheco Santos, V.; Tremiliosi-Filho, G.; *J. Electroanal. Chem.* **2003**, *395*, 554.
8. Schimidt, V. M.; Ianniello, R.; Pastor, E.; Gonzales, E. R.; *J. Phys. Chem.* **1996**, *100*, 17901.
9. Delime, F.; Léger, J. M.; Lamy, C.; *J. Appl. Electrochem.* **1999**, *29*, 1249.
10. Wang, Q.; Suna, G. Q.; Cao, L.; Jiang, L.H.; Wang, G. X.; Wang, S. L.; Yang, S. H.; Xina, Q.; *J. Power Sources* **2008**, *177*, 142.
11. Wu, G.; Swaidan, R.; Cui, G.; *J. Power Sources* **2007**, *172*, 180.
12. Suffredini, H. B.; Salazar-Banda, G. R.; Avaca, L. A.; *J. Power Sources* **2007**, *171*, 355.
13. Tsiakaras, P. E.; *J. Power Sources* **2007**, *171*, 107.
14. Freitas, R. G.; Santos, M. C.; Oliveira, R. T. S.; Bulhoes, L. O. S.; Pereira, E. C.; *J. Power Sources* **2006**, *158*, 164.
15. Lamy, C.; Lima, A.; LeRhun, V.; Delime, F.; Coutaceau, C.; Léger, J. M.; *J. Power Sources* **2002**, *105*, 283.
16. Lamy, C.; Belgsir, E. M.; Léger. J. M.; *J. Appl. Electrochem.* **2001**, *31*, 799.
17. Oliveira, R. T. S.; Marcussi, B.; Santos, M. C.; Tanimoto, S.; Bulhões, L. O. S.; Pereira, E. C.; *J. Power Sources* **2006**, *157*, 212.
18. Villullas, H. M.; Mattos Costa, F. I.; Bulhões, L. O. S.; *J. Phys. Chem. B* **2004**, *108*, 12898.
19. Profeti, L. P. R.; Simoes, F. C.; Olivi, P.; Kokoh, K. B.; Coutanceau, C.; Leger, J. M.; Lamy, C.; *J. Power Sources* **2006**, *158*, 1195.
20. Freitas, R. G.; Marchesi, L. F.; Oliveira, R. T. S.; Mattos-Costa, F. I.; Pereira, E. C.; Bulhoes, L. O. S.; Santos, M. C.; *J. Power Sources* **2007**, *171*, 373.
21. Freitas, R. G.; Oliveira, R. T. S.; Santos, M. C.; Bulhoes, L. O. S.; Pereira, E. C.; *Mater. Lett.* **2006**, *60*, 1906.
22. Burke, L. D.; Murphy, O. J.; *J. Electroanal. Chem.* **1979**, *101*, 351.
23. Lai, C. M.; Lin, J. C.; Hsueh, K. L.; Hwang, C. P.; Tsay, K. C.; Tsai, L. D.; Peng., Y. M.; *Int. J. Hydrogen Energy* **2007**, *32*, 4381.
24. Guo, J.; Sun, G.; Wu, Z.; Sun, S.; Yan, S.; Cao, L.; Yan, Y.; Su, D.; Xin, Q.; *J. Power Sources* **2007**, *172*, 666.
25. Chakraborty, D.; Chorkendorff, I.; Johannessen, T.; *J. Power Sources* **2007**, *173*, 110.
26. Huang, B.; Wang, S. R.; Liu, R. Z.; Wen, L.T.; *J. Power Sources* **2007**, *167*, 288.
27. Song, S.; Wang, G.; Zhou, W.; Zhao, X.; Sun, G.; Xin, Q.; Kontou, S.; Tsiakaras, P.; *J. Power Sources* **2005**, *140*, 103.
28. Xu, C.; Shen, P. K.; *J. Power Sources* **2005**, *142*, 27.
29. Boukamp, B. A.; *Solid State Ionics* **1986**, *18*, 136.
30. Dobholfer, K.; Metikos, M.; Ogumi, Z.; Gerisher, H.; *Ber. Bunsen-Ges. Phys. Chem.* **1978**, *82*, 1046.
31. Santos, M. C.; Terezo, A. J.; Fernandes, V. C.; Pereira, E. C.; Bulhoes, L. O. S.; *J. Solid State Electrochem.* **2005**, *9*, 91.
32. Santos, M. C.; Codognoto, L.; Tanimoto, S. T.; Calegaro, M. L.; Bulhoes, L. O. S.; *Appl. Surf. Sci.* **2006**, *253*, 1817.
33. Terezo, A. J.; Pereira, E. C.; *Mater. Lett.* **2002**, *53*, 339.
34. Savinova, E. R.; Hahn, F.; Alonso-Vante, N.; *Phys. Chem. Chem. Phys.* **2007**, *9,* 5693.
35. Pozniak, B.; Scherson, D. A.; *J. Am. Chem. Soc.* **2004**, *126*, 14696.
36. Markovic, N. M. In *Handbook of Fuel Cells: Fundamentals, Technology and Applications*; Vielstich, W.; Gasteiger, H. A.; Yokokawa, H., eds.; John Wiley & Sons: Chichester, 2003, vol. 2, p. 368.
37. Wieckowski, A.; Savinova, E. R.; Vayenas, C. G.; *Catalysis & Electrocatalysis at Nanoparticle Surfaces*, Marcel Dekker, Inc.: New York, 2003.
38. Farias, M. J. S.; Camara, G. A.; Tanaka, A. A.; *J. Solid State Electrochem.* **2007**, *11*, 1465.
39. Anjos, D. M.; Hahn, F.; Leger, J. M.; Kokoh, K. B.; Tremiliosi-Filho, G.; *J. Solid State Electrochem.* **2007**, *11*, 1567.

40. Bock, C.; Blankely, M. A.; MacDougall, B.; *Electrochim. Acta* **2005**, *50*, 2401.
41. Watanabe, M.; Motoo, S.; *J. Electroanal. Chem.* **1975**, *60*. 267.
42. Koper, M. T. M.; Lukkien, J. J.; Jansen, A. J.; van Santen, R. A.; *J. Phys. Chem. B* **1999**, *105*, 5522.
43. Igarashi, H.; Fujino, T.; Zhu, Y. M.; Uchida, H.; Watanabe, M.; *Phys. Chem. Chem. Phys.* **2001**, *3*, 306.
44. Massong, H.; Wang, H.; Samjeske, G.; Baltruschat, H.; *Electrochim. Acta* **2000**, *46*, 701.
45. Beden, B.; Kadirgan, F.; Lamy, C.; Leger, J. M.; *J. Electroanal. Chem.* **1989**, *127*. 75.
46. Mailard, F.; Eikerling, M.; Cherstiouk, O.V.; Schereier, S.; Savinova, E.; Stimming, U.; *Faraday Discuss.* **2004**, *125*, 357.
47. Chen, S.; Schell, M.; *J. Electroanal. Chem.* **1999**, *478*, 108.
48. Yang, L. X.; Allen, R. G.; Scott, K.; Christensen, P. A.; Roy, S.; *Electrochim. Acta* **2005**, *50*, 1217.
49. Wang, H; Jusys, Z.; Behm, R. J.; *Electrochim. Acta* **2009**, *54*, 6484.
50. Vigier, F.; Coutanceau, C. ; Hahn, F.; Belgsir, E. M.; Lamy, C.; *J. Electroanal. Chem.* **2004**, *563*, 81.
51. Souza, J. P. I.; Queiroz, S. Q.; Bergamaski, K.; Gonzalez, E. R.; Nart, F. C.; *J. Phys. Chem. B* **2002**, *106*, 9825.
52. Ianniello, R.; Schmidt, V. M.; Rodriguez, J. L.; Pastor, E.; *J. Electroanal. Chem.* **1999**, *471*, 167.
53. Camara, G. A.; Lima, R. B.; Iwasita, T.; *Electrochem. Commun*. **2004**, *6*, 812.
54. Camara, G. A.; Iwasita, T.; *J. Electroanal. Chem.* **2005**, *578*, 315.
55. Pereira, M. G.; Jimenez, M. D.; Elizalde, M. P.; Robledo, A. M.; Vante, N. A.; *Electrochim. Acta* **2004**, *49*, 3917.
56. Nagal, M.; Gonzalez, R. D.; *Ind. Eng. Chem. Prod. Res. Dev.* **1985**, *24*, 525.
57. Lin, R.; Luo, M. F.; Xin, Q.; Sun, G. Q.; *Catal. Lett.* **2004**, *93*, 139.
58. Bagotzky, V. S.; Vassilyew, Y. B.; *Electrochim. Acta* **1967**, *12*, 1323.
59. Santos, M. C.; Bulhoes, L. O. S.; *Electrochim. Acta* **2003**, *48*, 2607.
60. Melnick, R. E.; Palmore, G. T. R.; *J. Phys. Chem. B* **2001**, *105*, 9449.
61. Wu, G.; Li, L.; Xu, B. Q.; *Electrochim. Acta* **2004**, *50*, 1.
62. Nyikos, L.; Pajkossy, T.; *Electrochim. Acta* **1985**, *30*, 1533.

Submitted: November 2, 2010
Published online: June 16, 2011

FAPESP has sponsored the publication of this article.